Molecular Motion in Ultrathin Polystyrene Films: Dynamic Mechanical Analysis of Surface and Interfacial Effects

Kei-ichi Akabori, Keiji Tanaka,* Toshihiko Nagamura,* Atsushi Takahara,† and Tisato Kajiyama‡

Department of Applied Chemistry, Faculty of Engineering, Kyushu University, 6-10-1 Hakozaki, Higashi-ku, Fukuoka 812-8581, Japan

Received June 2, 2005; Revised Manuscript Received August 19, 2005

ABSTRACT: Dynamic mechanical analysis was successfully used, for the first time, to characterize polymer thin and ultrathin films supported on substrates. This method allowed us to uncover the effects of the free surface and the substrate interface on the segmental dynamics in polystyrene (PS) films with various thicknesses. As the film thickness decreased, the distribution of relaxation times for the segmental motion became broader, a change mainly due to surface and interfacial effects. Interestingly, PS ultrathin films sandwiched with SiO_x layers exhibited a relaxation process corresponding to the interfacial segmental motion in addition to that in the internal region of the films. The results obtained in this study imply that two contrasting effects exist: the effect of the free surface accelerates the segmental motion, whereas interfacial interactions produce the opposite effect.

Introduction

Thin and ultrathin polymer films have become widely utilized in such cutting-edge applications as nanocoatings, nanoadhesion and nanolubrication, biomaterials, and multilayer devices. Here, we define an ultrathin polymer film as one with a thickness comparable to, or less than, the chain dimension. In such ultrathin films, the chain conformation is no longer a random coil, and the ratio of the surface and interfacial area to the total volume becomes larger. Thus, the physical properties of these films are often different from those of the bulk materials.[1]

During the past decade, the thermal properties of ultrathin films of polymers deposited on substrates have been extensively studied by a great variety of techniques.[2−21] The general conclusion from these studies is that the glass transition temperature (T_g) in the ultrathin state deviates from the bulk value. If an attraction exists between the chains and the substrate, the T_g of such films increases over that in the bulk,[3,10,18−20] a change which implies that the substrate interface strongly restricts molecular motion in the films.[22−25] Otherwise, T_g is less than the bulk value, probably because of the presence of a surface layer[4,5,8−10,13,14,21] in which molecular motion is more active[26−40] and/or the confinement of chains into a narrow space.[41,42] This tendency was observed in polystyrene (PS) ultrathin films. Forrest, Dutcher et al. have presented interesting studies using free-standing PS ultrathin films.[43] Such films possess two free surfaces instead of a free surface and the substrate interface; thus, the T_g reduction from the bulk value was much more pronounced than that of the corresponding supported films.[43b] This result convincingly shows that the surface and interfacial effects should be crucial factors affecting the thermal properties of ultrathin polymer films. However, little information about segmental dynamics in these films is currently available.

Dielectric relaxation spectroscopy (DRS) is a well-established technique for examining molecular dynamics. It has already been applied to ultrathin films of various polymers; results from its use have shown that the relaxation time distribution, fragility, and T_g vary with decreasing film thickness.[9,44,45] However, in the case of DRS, a specimen needs to be sandwiched between two electrodes, meaning that the film does not possess free surface. Thus, the reported anomalous dynamics induced by ultrathinning could arise from an interfacial interaction with the electrodes and/or from the chain confinement effect. Of course, if the electrodes did not perfectly cover the specimen, a surface effect would appear in addition to the two effects above.[46] In such a case, it is hard to separate each relevant factor from the mixture.

So far, a few additional methods have been proposed to study the issue. By optical birefringence measurements, Schwab et al. have clarified the relaxation dynamics of PS ultrathin films in which the surface had been rubbed.[13] Although they clearly showed a surface effect on the thin film dynamics, in their experiment, the chains in the films were stretched by the rubbing. Thus, the results they obtained cannot be directly transferred to the situation in pristine films. Further, Forrest et al. have applied photon correlation spectroscopy to free-standing PS ultrathin films and have claimed that the shape of the relaxation function in the films was similar to that of the bulk sample.[43c] The latter authors have also used a quartz crystal microbalance (QCM) for measurements on PS ultrathin films on substrates.[43c] While QCM provided the relation between the temperature and relaxation time, it did not reveal the distribution of relaxation times.

Hence, a different experimental technique is needed, one which would permit a systematic study of the surface and interfacial effects on the segmental dynamics in ultrathin polymer films. One possibility might be dynamic viscoelastic measurements that have been widely used to study molecular motion in bulk polymer

† Institute for Materials Chemistry and Engineering, Kyushu University.
‡ Kyushu University.
* Corresponding authors: Tel +81-92-642-3560 (K.T.), +81-92-642-3558 (T.N.); Fax +81-92-651-5606; e-mail k-tanaka@cstf.kyushu-u.ac.jp (K.T.), nagamura@cstf.kyushu-u.ac.jp (T.N.).

10.1021/ma051143e CCC: $30.25
Published on Web 10/14/2005

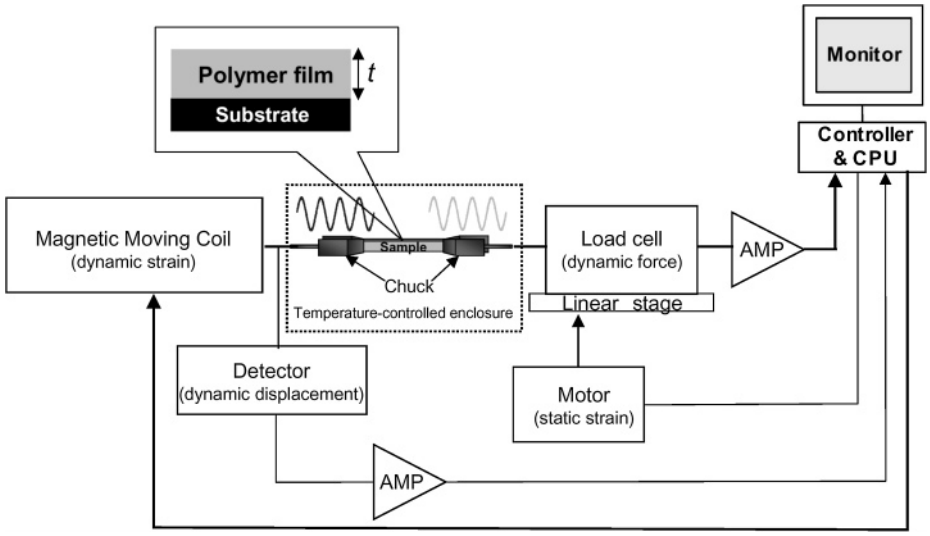

Figure 1. Schematic representation of the experimental setup for DMA.

films.[47] If this bulk technique is sensitive enough for the thin and ultrathin films, several intriguing issues could be addressed. First, both the relation between relaxation time and temperature and the distribution of relaxation times would be accessible. Second, when the measured specimen is in the most practical form of a spin-coated film, the film surface would be free. This feature comprises a significant advantage over DRS. Third, the surface of the substrate could be chemically and physically modified, enabling a systematical study of the interfacial effect. Finally, the film surface could be capped, like a specimen for DRS. In this case, the film would possess two interfaces instead of the free surface and the substrate interface. Hence, the effects of the surface and substrate interface on the segmental dynamics in polymer thin and ultrathin films could be clarified. In addition, it should be noted that dynamic mechanical analysis is one of the methods to measure T_g that is recommended by the American Standard for Testing Materials.

In this study, we first present an evaluation of the validity of dynamic mechanical analysis for PS thin and ultrathin films supported on substrates. Then, we discuss in detail the surface and interfacial effects on thermal molecular motion in those films.

Experimental Section

Monodisperse PSs with number-average molecular weight (M_n) of 53.4K and 1.46M were used in our experiments. The values of ($2R_g$) (R_g is the radius of gyration of an unperturbed chain) were calculated to be 12.6 and 66 nm, respectively. The bulk glass transition temperature (T_g^b) was measured by differential scanning calorimetry (DSC) under a dry nitrogen purge at a heating rate of 10 K min^{-1}. The values for PS53.4K and PS1.46M were 376 and 378 K, respectively. PS films with various thicknesses were spin-coated from toluene solutions onto commercially available polyimide (PI) film substrates with a thickness of 7.5 μm. In addition, a PI film covered with a 20 nm layer of SiO_x was used as an alternative substrate, being chosen for its resemblance to a Si wafer covered with the native oxide layer. First, Si was evaporated in a vacuum chamber and deposited onto a PI film. Then, the deposited Si layer was oxidized under the ambient atmosphere for a week, the oxidation being confirmed by spectroscopic measurements. In addition, to eliminate the effect of the free surface, some of the PS films on the SiO_x substrates were capped by SiO_x layers following the above-mentioned vacuum evaporation procedure[43b,48,49] and the lamination method proposed by Sharp and Forrest.[46] In the later method, a PS film with a thickness of ~20 nm was spin-coated on a SiO_x substrate. Also, a PS film with a similar thickness was spin-coated on a single crystal of sodium chloride (NaCl), in which the surface was covered with a deposited SiO_x layer. Then, one was put on the other so that the PS surfaces stand face-to-face. After annealing at 393 K for 8 h to heal the interface, it was immersed into a pure water bath, or wet by water droplets, to dissolve the NaCl crystal. This was so-called a laminated film hereafter. To remove residual solvent molecules and to eliminate stress imposed by the preparation procedure, the PS films were dried at room temperature for more than 24 h and then annealed at 423 K above the T_g^b for at least 24 h in a vacuum oven. After annealing, the films were cooled to room temperature at a rate of 0.5 K min^{-1}. Using an optical microscope, we confirmed that dewetting of PS on the substrate did not take place even after the annealing treatment.

The thermal molecular motion of the PS thin and ultrathin films was examined by dynamic mechanical analysis (DMA) using a Rheovibron DDV-01FP (A&D Co., Ltd.) tester. Figure 1 shows the experimental setup for DMA. For the measurement, a sample with a width of 3 mm and a length of 30 mm was held at both ends by two chucks, and static strain was applied. Then, sinusoidal strain was imposed to the sample within the linear response regime. The measurements were carried out at a heating rate of 1 K min^{-1} under a dry nitrogen atmosphere.

Results and Discussion

In general, DMA has been accepted as a powerful method to study the relaxation behavior of bulk samples.[47] However, previous to these experiments, we did not know whether the technique was sensitive enough to be used with polymer thin and ultrathin films. To answer this question, we conducted a dynamic viscoelastic measurement for thin and ultrathin PS films supported on substrates. Figure 2 shows the temperature dependence of the loss modulus (E'') for PS films of various thicknesses on PI, together with the data for a control PI substrate. For reasons of space, only the data at the frequency of 11 Hz are presented, although we took data at several other frequencies. In the case of the 226 nm thick film, we succeeded in observing an α_a absorption peak corresponding to the segmental motion at around 380 K on the temperature−E'' curve. This result is in good accordance with the bulk data. Because the volume ratio of the PS phase to that of the total system fell, the intensity of the α_a relaxation

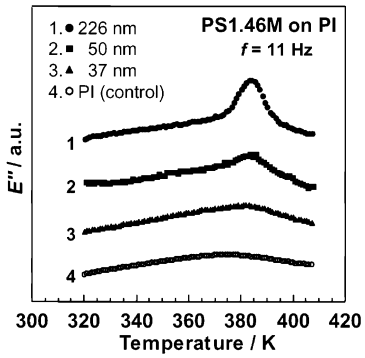

Figure 2. Temperature dependence of the loss modulus (E'') for PS1.46M thin and ultrathin films coated on PI substrates. The data for a control PI are also shown.

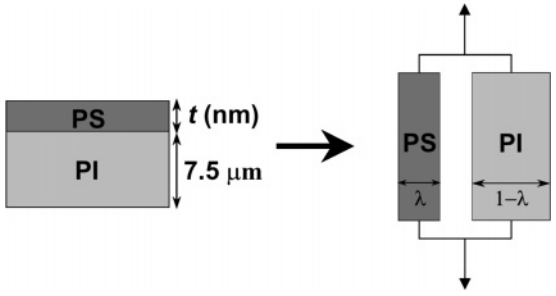

Figure 3. Schematic representation of Takayanagi's parallel model for PS on PI.

peak for the PS decreased as the films became thinner. However, as explained below, even the 37 nm thick film appeared to generate sufficient of a relaxation peak to which we could apply a mechanical model analysis to the raw data to extract the contribution from the PS phase.

Figure 3 illustrates Takayanagi's parallel model, in which the dynamic strain ($\Delta\epsilon$) is everywhere constant.[47] Here, t and λ are the thickness in nanometers and volume fraction of PS, respectively. On the basis of this model, we can formulate the E'' for a PS film coated on PI (E''_{all}) by[50]

$$\Delta F = \Delta\sigma_{all}S_{all} = \Delta\sigma_{PS}S_{PS} + \Delta\sigma_{PI}S_{PI}, \quad S_{all} = S_{PS} + S_{PI} \tag{1a}$$

$$E^* = \Delta\sigma/\Delta\epsilon, \quad E^* = E' + iE'' \tag{1b}$$

$$E^*_{all} = \{\Delta\sigma_{PS}S_{PS}/S_{all} + \Delta\sigma_{PI}(S_{all} - S_{PS})/S_{all}\}/\Delta\epsilon = \lambda E^*_{PS} + (1-\lambda)E^*_{PI} \tag{1c}$$

$$E'_{all} = \lambda E'_{PS} + (1-\lambda)E'_{PI}, \quad E''_{all} = \lambda E''_{PS} + (1-\lambda)E''_{PI} \tag{1d}$$

where S, ΔF, $\Delta\sigma$, E^*, and E' are the cross-sectional area, dynamic force, dynamic stress, complex modulus, and storage modulus, respectively.

$$E''_{PS} = \{(7500 + t)E''_{all} - 7500E''_{PI}\}/t \tag{2}$$

This type of substrate subtraction was applied to both the PS films on SiO_x substrates and to the ones sandwiched between the SiO_x layers. The errors of E''_{PS} so obtained were within 5% and 10% for thin and ultrathin films.

Figure 4 shows the temperature dependence of the background-subtracted E'' as a function of frequency for

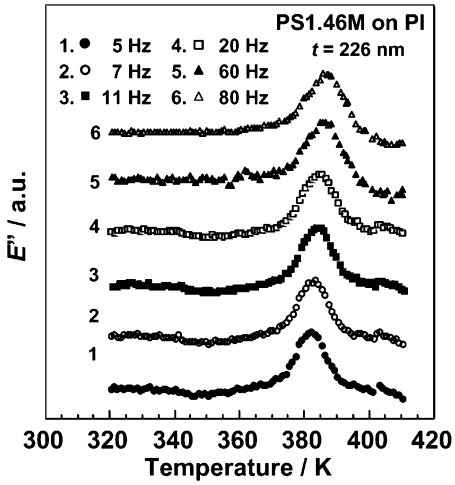

Figure 4. Temperature dependence of E'' as a function of frequency for a 226 nm thick PS1.46M film coated on a PI substrate, after baseline correction. The $T_g{}^b$ value measured by DSC was 378 K.

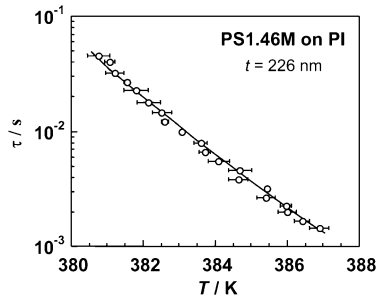

Figure 5. Temperature dependence of the relaxation time (τ) for the α_a process in a 226 nm thick PS1.46M film coated on a PI substrate. The solid curve denotes the prediction of the Vogel−Fulcher equation using bulk parameters.

the 226 nm thick PS film on PI. Since the M_n for the PS used was 1.46M, the film was much thicker than the chain dimension of 66 nm. On each temperature−E'' curve, we noted the α_a absorption peak in the temperature range from 380 to 390 K. The peak position shifted to higher temperature with increasing frequency.

The relation between peak temperature and measuring frequency (f) for the α_a relaxation process can be simply converted to the temperature dependence of relaxation time (τ) via eq 3.

$$(2\pi f)\tau = 1 \tag{3}$$

Figure 5 shows the relation between temperature and τ for the α_a relaxation process in the 226 nm thick PS1.46M film on PI. The error bars in Figure 5 denote the standard deviation of the relaxation temperature from seven independent measurements. We compared the film results with the bulk behavior, which we obtained by the Vogel−Fulcher (VF) equation.[51]

$$\tau = \tau_0 \exp\{B/(T - T_v)\} \tag{4}$$

Here, T_v is the so-called Vogel temperature, at which the viscosity diverges to infinity; it is generally equal to $T_g - 50$. The parameters τ_0 and B are the characteristic time related to molecular vibration and the activation temperature, respectively. Using the T_v value of 328 K, given by $T_g - 50$, and the published B value for bulk PS,[9c] we drew the solid curve which was in good agreement with the experimental results shown in

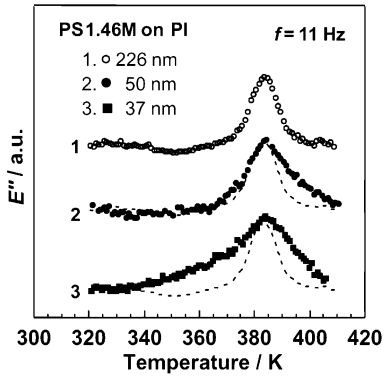

Figure 6. Temperature dependence of E'' for PS1.46M thin and ultrathin films on PI, after baseline correction. The data for the ultrathin films, plotted as filled symbols, were rescaled to have the same peak height as the 226 nm thick film. To make a comparison between thin and ultrathin films easier, the temperature absorption for the 226 nm thick film was drawn as a dashed curve superimposed on the data for the ultrathin films.

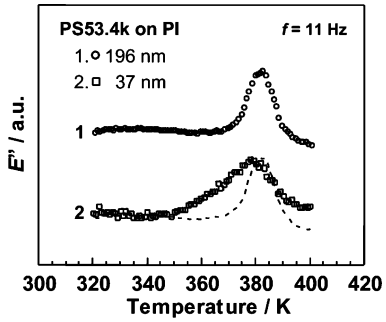

Figure 7. Temperature dependence of E'' for PS53.4K thin films on PI, after baseline correction. The data for the 37 nm thick film was rescaled to have the same peak height as the 196 nm thick film. To make a comparison between two films easier, the temperature absorption for the 196 nm thick film was drawn as a dashed curve superimposed on the data for the 37 nm thick film.

Figure 5. The segmental mobility in a PS film with a thickness of about 200 nm supported on a solid substrate is generally equal to the bulk behavior.[1] Hence, the data shown in Figures 4 and 5 are quite reasonable, and on that basis, we can claim that DMA still works well for polymer films with thicknesses of a few hundred nanometers.

We then applied the method to thinner films. Figure 6 shows the temperature dependence of the background-subtracted E'' at 11 Hz for the PS1.46M thin and ultrathin films spin-coated on the PI substrates. To facilitate comparison, we rescaled the variable E'' for the ultrathin films with thicknesses of 50 and 37 nm to have the same peak height as that of the 226 nm thick film. In addition, we superimposed the data for the 226 nm thick film, shown as a dashed curve, on the ultrathin film data. The α_a absorption peak was clearly observed even for the films that were thinner than the chain dimension. However, the ultrathin films exhibited a broader relaxation peak toward both lower and higher temperatures than did the 226 nm thick film. This result indicated that the distribution of the relaxation times for the α_a process broadened as the film thickness decreased. However, our explanation should be couched in terms of the surface and interfacial effects and/or the chain confinement effect.

To discuss whether the chain confinement is important to the peak broadening, we examined the temperature dependence of E'' for PS53.4K films with thicknesses of 196 and 37 nm on PI substrates. Figure 7 shows the result. In the case of an unperturbed PS53.4K chain, the $2R_g$ value was calculated to be 12.6 nm, a value much less than the film thicknesses. Thus, we expect that the chain confinement effect should be unimportant for both films. Nevertheless, the width of the α_a absorption peak for the 37 nm thick film was much broader than that for the 196 nm thick film. Hence, it is plausible that the thinning-induced peak broadening is mainly caused by the surface and interfacial effects. In other words, the faster and slower relaxation times might be due to the segmental motion in the surface and interfacial regions, respectively. If, as the film thickness decreases, the peak finally splits into three peaks that arise from the surface, the internal region, and the interfacial region, a further discussion about the segmental dynamics at a different depth in the ultrathin film becomes possible. However, such splitting was not found for the PS films in the thickness range studied. In addition, the thinning-induced peak broadening for the PS53.4K film was asymmetric; specifically, the surface effect was more noticeable than the interfacial one. Such was not the case for the 37 nm thick film of PS1.46M in Figure 6. The number density of the chain ends is proportional to a reciprocal number of M_n. Taking into account that the chain ends preferentially segregate to the surface to minimize free energy at the air/polymer interface, we believe that the segmental motion in the surface region becomes faster for a film with smaller M_n.[27a,b] Although the surface dynamics is not so simple in reality, the asymmetric peak broadening observed in Figure 7 might be qualitatively understood on the basis of the surface segregation of chain ends.

Here, we should discuss the mobility gradient in the films. Recently, Ellison and Torkelson, using a fluorescence/multilayer method, concluded that the T_g depression of a thin film was mainly caused by the presence of a surface region, in which the segmental mobility was enhanced, and that, because of the surface effect, the T_g began to fall at a critical thickness of ~50 nm.[8c] In addition, the T_g value in the 10 nm thick layer of the outermost surface was lower than the T_g^b by 30 K and gradually reached the T_g^b at a depth of about 30 nm from the outermost surface. We noted a similar tendency in our mechanical relaxation test. In the case of the 37 nm thick film, E'' started to rise at around 340 K, a temperature which was lower than that of the corresponding bulk value by ~30 K. Furthermore, an independent experiment we conducted using scanning force microscopy revealed that the surface T_g in the film of PS with M_n of 1.0M was almost 340 K.[27b,c] Therefore, it is conceivable that the α_a process peak broadening on the lower temperature side reflects a mobility gradient in the surface region.

We now come to the interfacial effect on molecular motion in the PS thin and ultrathin films. For this analysis, we examined two kinds of PS films. The first comprises the PS1.46M films spin-coated on SiO_x substrates. This system resembles that of a PS film on a Si wafer with a native oxide layer and is the most studied case so far. The second is the PS1.46M film sandwiched between SiO_x layers. In this case, the films do not possess a free surface; instead, they possess two interfaces with the SiO_x layers. To keep the upper interface during the measurement, we set the thickness of the

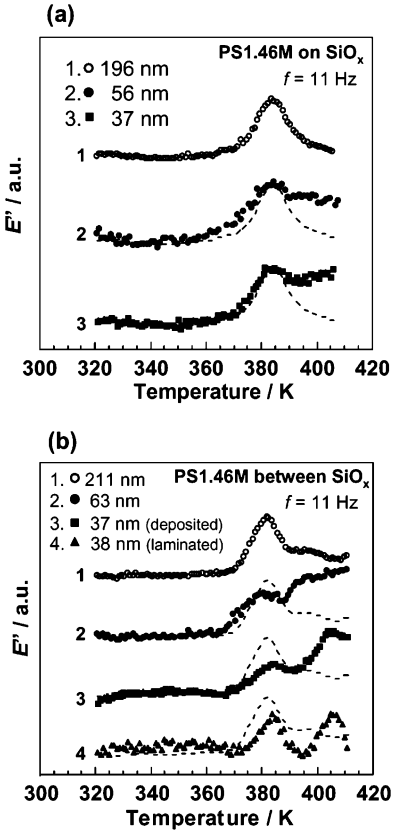

Figure 8. Temperature dependence of E'' for PS1.46M thin and ultrathin films, after baseline correction: (a) on SiO_x substrates and (b) sandwiched between SiO_x layers.

capped SiO_x layer to be about 20 nm. Figure 8 shows the temperature dependence of background-subtracted E'' as a function of thickness for the PS1.46M films (a) on the SiO_x substrate and (b) between the SiO_x layers. The values of E'' for the ultrathin films were again arbitrarily rescaled to have the same peak height as that for the 200 nm thick films. In the case of the PS1.46M on the SiO_x, we clearly saw the α_a absorption peak, even for the ultrathin films with thicknesses of 56 and 37 nm.

First, we compared the data sets for the PS1.46M films on the SiO_x and on the PI substrates; these appear in Figures 8a and 6. The temperature absorption curve for the 196 nm thick film on the SiO_x was in good accordance with that for the 226 nm thick film on the PI, a result suggesting that the interfacial effect on the α_a relaxation process is negligible in this thickness region. More precisely, even if the surface and interfacial effects on molecular motion exist, they are not detectable for this thickness range. On the other hand, for the thinner films, the shape of the α_a absorption peak depended on which substrate was used. We noted an obvious difference between the ultrathin films on the SiO_x and PI on the higher temperature side of the peak. For the ultrathin films on the PI, E'' monotonically decreased with increasing temperature, as shown in Figure 6. In contrast, in the case of the ultrathin films on the SiO_x substrates, E'' slightly decreased, and then remained almost constant, or increased again after the peak, as shown in Figure 8a. This result means that the fractional amount of slower relaxation times in the ultrathin films on the SiO_x is larger than that in the corresponding films on the PI. Thus, it seems most likely that the chains that are in contact with the SiO_x layer are less mobile than those next to the PI. This trend was more marked for the ultrathin PS films sandwiched between the SiO_x layers. At a later point, we will discuss this issue, as well as the characteristics of the lower side of the peak, in more detail. For the ultrathin films on the PI, the peak broadening on the lower temperature side became more marked with decreasing thickness (Figure 6). Postulating that the surface segmental motion might be more detectable with decreasing thickness due to the larger surface-to-volume ratio, we consider this result to be reasonable. However, we did observe a strange thickness dependence of the broadening for the ultrathin films on the SiO_x (Figure 8a). In the case of the 56 nm thick film, we noted the peak broadening on the lower temperature side, but on the other hand, we did not observe it for the thinner, 37 nm thick film. These findings may indicate that the molecular motion in the surface region is inhibited by a restriction from the interface, if the interfacial effect is strong. The same trend was also observed by Ellison and Torkelson.[8c]

We will now discuss the segmental motion in the PS films sandwiched between the SiO_x layers. Even in the case of the 211 nm thick film, we did see an additional shoulder on the higher temperature side of the α_a relaxation peak, as shown in Figure 8b. As the film thinned, the high-temperature shoulder evolved and eventually became a clear peak. Since the presence of the additional peak for the 37 nm thick film sandwiched between the SiO_x layers depended on the frequency employed, it is clear that the peak derived from a relaxation process. In addition, in the case of the sandwiched films, the relaxation peak did not broaden on the lower temperature side, even though the films became thinner. This result can be easily understood by taking into account the film geometry. In other words, the free surface disappeared under the capping SiO_x layer, and the interfacial region with the SiO_x layer doubled. On the basis of the results mentioned above, we suggest that the main and additional peaks observed at the lower and higher temperature regions should be assigned respectively to the α_a relaxation processes in the internal phase and the interfacial layer.

However, at the moment, we are not able to deny the possibility that the sandwiched films were thermally damaged by the vacuum-deposition procedure,[52] although such damage was not visible in the microscopic observations. Hence, to investigate this likelihood, we prepared a PS1.46M ultrathin film sandwiched with SiO_x layers by laminating two PS films on SiO_x layers.[46] In this case, the film should not have suffered any thermal damage. The result for the sandwiched film prepared by the lamination is shown in Figure 8b and clearly shows the additional peak in the higher temperature region. Although the intensity of the additional peak was different in the two sandwiched films prepared by different methods, their temperature regions seemed to be similar. Since the additional peak was observed only for the ultrathin PS film sandwiched with SiO_x layers, it is likely that the peak on the higher temperature side arose from an interfacial relaxation process and is not an experimental artifact.

Figure 9 shows the temperature dependence of τ for the α_a relaxation processes in the internal and interfacial regions of the ultrathin PS1.46M film sandwiched between the SiO_x layers. Since it was hard to distinguish the temperature$-\tau$ relations between the vacuum-

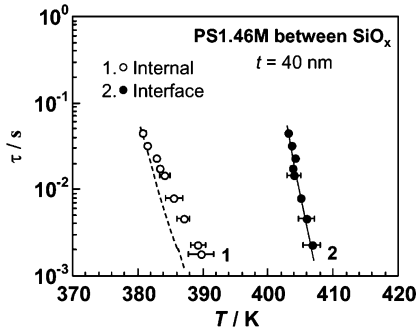

Figure 9. Temperature dependence of τ for α_a relaxation processes in internal and interfacial regions of the PS1.46M ultrathin films sandwiched between SiO_x layers. The average thickness is about 40 nm. The dashed curve denotes the prediction of the Vogel−Fulcher equation using bulk parameters, whereas the solid curve is the best-fit one by VF equation for the interfacial α_a process.

deposited and laminated films, each data point was averaged over six independents including both vacuum-deposited and laminated films. The average thickness was about 40 nm. For a comparison, we have also drawn the bulk data obtained by the VF equation as a dashed curve. Even in the case of the internal phase, the temperature dependence of τ slightly deviated from the bulk data. This discrepancy might be due to an effect of chain confinement, which appeared in the high molecular weight PS ultrathin films.[42b] However, Figure 9 shows that the temperature−τ relation in the interfacial layer was definitely different from that in the internal region. Since the interfacial α_a relaxation process seems to be independent of the internal one, the data set from the interfacial regions was fitted by the VF equation with a single Vogel temperature, as drawn by a solid curve in the figure. The T_v so obtained was 369 ± 4 K. Now, T_g is generally accepted to equal (T_v + 50) K. So, even for this simplified case, the value T_g in the interfacial layer should be 419 ± 4 K, a temperature higher than the T_g^b value of 378 K. Although the plausibility of this quantitative estimation for the interfacial T_g value merits further discussion, it is evident that the segmental mobility at the interface with the SiO_x layer is depressed in comparison with that for the bulk.

Conclusions

Thermal molecular motion in PS thin and ultrathin films supported on substrates has, for the first time, been studied by dynamic viscoelastic measurement. In the case of a PS thin film with a thickness of ~200 nm, we clearly observed an α_a relaxation process corresponding to the segmental motion but did not see a deviation from the bulk behavior. For thinner films, the relaxation time distribution for the α_a process became broader, probably due to a mobility gradient in the surface and interfacial regions. When we sandwiched a PS ultrathin film between the SiO_x layers, another relaxation process, in addition to the original α_a process, appeared at a higher temperature that we assigned to the interfacial α_a relaxation process. These results indicate that segmental mobility in PS ultrathin films coated on substrates is strongly affected by the free surface and the substrate interface.

Acknowledgment. This research was partly supported by a Grant-in-Aid from the 21st century COE program "Functional Innovation of Molecular Informatics" and from Scientific Research A (14205122) from the Ministry of Education, Science, Sports, and Culture, Japan.

References and Notes

(1) Forrest, J. A.; Jones, R. A. L. In *Polymer Surfaces, Interfaces and Thin Films*; Karim, A., Kumar, S., Eds.; World Scientific: Singapore, 2000.
(2) (a) Reiter, G. *Europhys. Lett.* **1993**, *23*, 579. (b) Reiter, G. *Macromolecules* **1994**, *27*, 3046. (c) Reiter, G. *Eur. Phys. J. E* **2002**, *8*, 251.
(3) (a) Orts, W. J.; van Zanten, J. H.; Wu, W. L.; Satija, S. K. *Phys. Rev. Lett.* **1993**, *71*, 867. (b) Wallace, W. E.; van Zanten, J. H.; Wu, W. L. *Phys. Rev. E* **1995**, *52*, R3329. (c) Pochan, D. J.; Lin, E. K.; Satija, S. K.; Wu, W. L. *Macromolecules* **2001**, *34*, 3041.
(4) (a) Keddie, J. L.; Jones, R. A. L.; Cory, R. A. *Europhys. Lett.* **1994**, *27*, 59. (b) Keddie, J. L.; Jones, R. A. L. *Isr. J. Chem.* **1995**, *35*, 21. (c) Kawana, S.; Jones, R. A. L. *Phys. Rev. E* **2001**, *63*, 021501.
(5) DeMaggio, G. B.; Frieze, W. E.; Gidley, D. W.; Zhu, M.; Hristov, H. A.; Yee, A. F. *Phys. Rev. Lett.* **1997**, *78*, 1524.
(6) (a) Frank, B.; Gast, A. P.; Russell, T. P.; Brown, H. R.; Hawker, C. *Macromolecules* **1996**, *29*, 6531. (b) Tsui, O. K. C.; Russell, T. P.; Hawker, C. J. *Macromolecules* **2001**, *34*, 5535.
(7) (a) Müller-Buschbaum, P.; Vanhoorne, P.; Scheumann, V.; Stamm, M. *Europhys. Lett.* **1997**, *40*, 655. (b) Müller-Buschbaum, P.; Gutmann, J. S.; Lorenz, C.; Schmitt, T.; Stamm, M. *Macromolecules* **1998**, *31*, 9265. (c) Kuhlmann, T.; Kraus, J.; Müller-Buschbaum, P.; Schubert, D. W.; Stamm, M. *J. Non-Cryst. Solids* **1998**, *235−237*, 457.
(8) (a) Hall, D. B.; Torkelson, J. M. *Macromolecules* **1998**, *31*, 8817. (b) Ellison, C. J.; Kim, S. D.; Hall, D. B.; Torkelson, J. M. *Eur. Phys. J. E* **2002**, *8*, 155. (c) Ellison, C. J.; Torkelson, J. M. *Nat. Mater.* **2003**, *2*, 695.
(9) (a) Fukao, K.; Miyamoto, Y. *Europhys. Lett.* **1999**, *46*, 649. (b) Fukao, K.; Miyamoto, Y. *Phys. Rev. E* **2000**, *61*, 1743. (c) Fukao, K.; Miyamoto, Y. *Phys. Rev. E* **2001**, *64*, 011803.
(10) (a) Fryer, D. S.; Nealey, P. F.; de Pablo, J. J. *Macromolecules* **2000**, *33*, 6439. (b) Fryer, D. S.; Peters, R. D.; Kim, E. J.; Tomaszewski, J. E.; de Pablo, J. J.; Nealey, P. F.; White, C. C.; Wu, W. L. *Macromolecules* **2001**, *34*, 5627.
(11) (a) Tseng, K. C.; Turro, N. J.; Durning, C. J. *Phys. Rev. E* **2000**, *61*, 1800. (b) Tseng, K. C.; Turro, N. J.; Durning, C. J. *Polymer* **2000**, *41*, 4751.
(12) Ge, S.; Pu, Y.; Zhang, W.; Rafailovich, M.; Sokolov, J.; Buenviaje, C.; Buckmaster, R.; Overney, R. M. *Phys. Rev. Lett.* **2000**, *85*, 2340.
(13) (a) Schwab, A. D.; Agra, D. M. G.; Kim, J. H.; Kumar, S.; Dhinojwala, A. *Macromolecules* **2000**, *33*, 4903. (b) Agra, D. M. G.; Schwab, A. D.; Kim, J. H.; Kumar, S.; Dhinojwala, A. *Europhys. Lett.* **2000**, *51*, 655.
(14) (a) Tsui, O. K. C.; Zhang, H. F. *Macromolecules* **2001**, *34*, 9139. (b) Xie, F.; Zhang, H. F.; Lee, F. K.; Du, B.; Tsui, O. K. C.; Yokoe, Y.; Tanaka, K.; Takahara, A.; Kajiyama, T.; He, T. *Macromolecules* **2002**, *35*, 1491.
(15) Masson, J. L.; Green, P. F. *Phys. Rev. E* **2002**, *65*, 031806.
(16) (a) Efremov, M. Y.; Warren, J. T.; Olson, E. A.; Zhang, M.; Kwan, A. T.; Allen, L. H. *Macromolecules* **2002**, *35*, 1481. (b) Efremov, M. Y.; Olson, E. A.; Zhang, M.; Zhang, Z.; Allen, L. H. *Macromolecules* **2004**, *37*, 4607.
(17) (a) Kanaya, T.; Miyazaki, T.; Watanabe, H.; Nishida, K.; Yamano, H.; Tasaki, S.; Bucknall, D. B. *Polymer* **2003**, *44*, 3769. (b) Miyazaki, T.; Nishida, K.; Kanaya, T. *Phys. Rev. E* **2004**, *69*, 022801.
(18) Keddie, J. L.; Jones, R. A. L.; Cory, R. A. *Faraday Discuss.* **1994**, *98*, 219.
(19) (a) Grohens, Y.; Brogly, M.; Labbe, C.; David, M. O.; Schultz, J. *Langmuir* **1998**, *14*, 2929. (b) Grohens, Y.; Hamon, L.; Reiter, G.; Soldera, A.; Holl, Y. *Eur. Phys. J. E* **2002**, *8*, 217.
(20) van Zanten, J. H.; Wallace, W. E.; Wu, W. L. *Phys. Rev. E* **1996**, *53*, R2053.
(21) Prucker, O.; Christian, S.; Bock, H.; Rühe, J.; Frank, C. W.; Knoll, W. *Macromol. Chem. Phys.* **1998**, *199*, 1435.
(22) (a) Zheng, X.; Sauer, B. B.; Van Alsten, J. G.; Schwarz, S. A.; Rafailovich, M. H.; Sokolov, J.; Rubinstein, M. *Phys. Rev. Lett.* **1995**, *74*, 407. (b) Zheng, X.; Rafailovich, M. H.; Sokolov, J.; Strzhemechny, Y.; Schwarz, S. A.; Sauer, B. B.; Rubinstein, M. *Phys. Rev. Lett.* **1997**, *79*, 241.

(23) Torres, J. A.; Nealey, P. F.; de Pablo, J. J. *Phys. Rev. Lett.* **2000**, *85*, 3221.
(24) (a) Long, D.; Lequeux, F. *Eur. Phys. J. E* **2001**, *4*, 371. (b) Merabia, S.; Sotta, P.; Long, D. *Eur. Phys. J. E* **2004**, *15*, 189.
(25) Ngai, K. L. *Eur. Phys. J. E* **2003**, *12*, 93.
(26) Meyers, G. F.; DeKoven, B. M.; Seitz, J. T. *Langmuir* **1992**, *8*, 2330.
(27) (a) Tanaka, K.; Taura, A.; Ge, S. R.; Takahara, A.; Kajiyama, T. *Macromolecules* **1996**, *29*, 3040. (b) Tanaka, K.; Takahara, A.; Kajiyama, T. *Macromolecules* **2000**, *33,* 7588. (c) Tanaka, K.; Hashimoto, K.; Kajiyama, T.; Takahara, A. *Langmuir* **2003**, *19,* 6573.
(28) Jean, Y. C.; Zhang, R.; Cao, H.; Yuan, J. P.; Huang, C. M.; Nielsen, B.; Asoka-Kumar, P. *Phys. Rev. B* **1997**, *56*, R8459.
(29) (a) Boiko, Y. M.; Prud'homme, R. E. *J. Polym. Sci., Part B: Polym. Phys.* **1998**, *36*, 567. (b) Guérin, G.; Mauger, F.; Prud'homme, R. E. *Polymer* **2003**, *44*, 7477.
(30) Hammerschmidt, J. A.; Gladfelter, W. L.; Haugstad, G. *Macromolecules* **1999**, *32,* 3360.
(31) Zaporojtchenko, V.; Strunskus, T.; Erichsen, J.; Faupel, F. *Macromolecules* **2001**, *34,* 1125.
(32) Kerle, T.; Lin, Z.; Kim, H. C.; Russell, T. P. *Macromolecules* **2001**, *34*, 3484.
(33) (a) Wallace, W. E.; Fischer, D. A.; Efimenko, K.; Wu, W. L.; Genzer, J. *Macromolecules* **2001**, *34*, 5081. (b) Wu, W. L.; Sambasivan, S.; Wang, C. Y.; Wallace, W. E.; Genzer, J.; Fischer, D. A. *Eur. Phys. J. E* **2003**, *12*, 127.
(34) (a) Kawaguchi, D.; Tanaka, K.; Takahara, A.; Kajiyama, T. *Macromolecules* **2001**, *34*, 6164. (b) Kawaguchi, D.; Tanaka, K.; Kajiyama, T.; Takahara, A.; Tasaki, S. *Macromolecules* **2003**, *36*, 1235.
(35) Fischer, H. *Macromolecules* **2002**, *35*, 3592.
(36) Bliznyuk, V. N.; Assender, H. E.; Briggs, G. A. D. *Macromolecules* **2002**, *35*, 6613.
(37) Jones, R. A. L. *Nat. Mater.* **2003**, *2*, 645.
(38) Weber, R.; Grotkopp, I.; Stettner, J.; Tolan, M.; Press, W. *Macromolecules* **2003**, *36*, 9100.
(39) Teichroeb, J. H.; Forrest, J. A. *Phys. Rev. Lett.* **2003**, *91*, 016104.
(40) Sasaki, T.; Shimizu, A.; Mourey, T. H.; Thurau, C. T.; Ediger, M. D. *J. Chem. Phys.* **2003**, *119*, 8730.
(41) Ngai, K. L.; Rizos, A. K.; Plazek, D. J. *J. Non-Cryst. Solids* **1998**, *235–237*, 435.
(42) (a) Dalnoki-Veress, K.; Forrest, J. A.; de Gennes, P. G.; Dutcher, J. R. *J. Phys. IV* **2000**, *10*, 221. (b) Dalnoki-Veress, K.; Forrest, J. A.; Murray, C.; Gigault, C.; Dutcher, J. R. *Phys. Rev. E* **2001**, *63*, 031801.
(43) (a) Forrest, J. A.; Dalnoki-Veress, K.; Stevens, J. R.; Dutcher, J. R. *Phys. Rev. Lett.* **1996**, *77*, 2002. (b) Forrest, J. A.; Dalnoki-Veress, K.; Dutcher, J. R. *Phys. Rev. E* **1997**, *56*, 5705. (c) Forrest, J. A.; Svanberg, C.; Révész, K.; Rodahl, M.; Torell, L. M.; Kasemo, B. *Phys. Rev. E* **1998**, *58*, R1226.
(44) (a) Cho, Y. K.; Watanabe, H.; Granick, S. *J. Chem. Phys.* **1999**, *110*, 9688. (b) Jeon, S.; Granick, S. *Macromolecules* **2001**, *34*, 8490. (c) Kojio, K.; Jeon, S.; Granick, S. *Eur. Phys. J. E* **2002**, *8*, 167.
(45) (a) Hartmann, L.; Kratzmüller, T.; Braun, H. G.; Kremer, F. *Macromol. Rapid Commun.* **2000**, *21*, 814. (b) Hartmann, L.; Gorbatschow, W.; Hauwede, J.; Kremer, F. *Eur. Phys. J. E* **2002**, *8*, 145. (c) Kremer, F.; Schönhals, A. In *Broadband Dielectric Spectroscopy*; Springer: Berlin, 2002.
(46) (a) Sharp, J. S.; Forrest, J. A. *Phys. Rev. Lett.* **2003**, *91*, 235701. (b) Sharp, J. S.; Forrest, J. A. *Eur. Phys. J. E* **2003**, *12*, S97.
(47) McCrum, N. G.; Read, B. E. In *Anelastic and Dielectric Effects in Polymeric Solids*; Dover: New York, 1967.
(48) Lambooy, P.; Salem, J. R.; Russell, T. P. *Thin Solid Films* **1994**, *252*, 75.
(49) On the basis of two experiments, we have tried to examine to what extent the temperature of the samples increases during the evaporation procedure. The first involved the use of a thermocouple, and in that case, the value obtained was ~333 K. Although this method can certainly detect radiative heat transfer, it may not reflect the effect of thermal SiO_x particles due to a larger heat capacity of the specimen. Hence, we used gallium (Ga) and indium (In), with melting points of 303 and 430 K, to probe the temperature. When we put Ga onto a substrate, we found that it was melted after the procedure. On the other hand, In did not melt. These results strongly imply that the samples were not heated above 430 K during the evaporation process.
(50) It is our assumption that the dynamic strain imposed is everywhere constant. When an interfacial phase, which has different mechanical properties between PS and PI, is formed, $\Delta\sigma_{all}S_{all}$ in eq 1a is supposed to be expressed by $\Delta\sigma_{PS}S_{PS} + \Delta\sigma_{PS'}S_{PS'} + \Delta\sigma_{PI}S_{PI}$, where PS′ denotes the interfacial phase. In a strict sense, we might have the fourth term arisen from the surface side as well. However, since we have not discuss the absolute values of E''_{PS}, we strongly believe that the parallel model can be used, especially, to subtract the contribution from the substrate. A limitation for using the parallel model is the case that moduli of polymer and substrate are extremely different, like, the buckling phenomenon is taken place. Such was not seen in this study, even though SiO_x was used as a substrate. In addition, for the moment, we are unable to perfectly deny a possibility that mechanical energy dissipation is in part arisen from the PS/PI interface. However, we have not discussed the absolute values of E''_{PS}. Hence, we believe that this point would not essentially alter the discussion. Of course, we should experimentally reveal to what extent the interfacial mechanical loss is important for the results. Thus, we have been now working on DMA for PS thin films on various substrates. The results will be reported in the near future.
(51) (a) Vogel, H. *Phys. Z.* **1921**, *22*, 645. (b) Fulcher, G. S. *J. Am. Ceram. Soc.* **1925**, *77*, 3701.
(52) Yan, S. *Macromolecules* **2003**, *36*, 339.

MA051143E